

This is the accepted manuscript made available via CHORUS. The article has been published as:

Measurement of the Target-Normal Single-Spin Asymmetry  
in Quasielastic Scattering from the Reaction  
 $^3\text{He}^{\uparrow}(e, e^{\prime})$

Y.-W. Zhang *et al.* (Jefferson Lab Hall A Collaboration)

Phys. Rev. Lett. **115**, 172502 — Published 22 October 2015

DOI: [10.1103/PhysRevLett.115.172502](https://doi.org/10.1103/PhysRevLett.115.172502)

# Measurement of the Target-Normal Single-Spin Asymmetry in Quasi-Elastic Scattering from the Reaction ${}^3\text{He}^\uparrow(e, e')$

Y.-W. Zhang,<sup>1,2</sup> E. Long,<sup>3</sup> M. Mihovilović,<sup>4</sup> G. Jin,<sup>5</sup> K. Allada,<sup>6</sup> B. Anderson,<sup>3</sup> J. R. M. Annand,<sup>7</sup> T. Averett,<sup>8,\*</sup> C. Ayerbe-Gayoso,<sup>8</sup> W. Boeglin,<sup>9</sup> P. Bradshaw,<sup>8</sup> A. Camsonne,<sup>6</sup> M. Canan,<sup>10</sup> G. D. Cates,<sup>5</sup> C. Chen,<sup>11</sup> J. P. Chen,<sup>6</sup> E. Chudakov,<sup>6</sup> R. De Leo,<sup>12</sup> X. Deng,<sup>5</sup> A. Deur,<sup>6</sup> C. Dutta,<sup>13</sup> L. El Fassi,<sup>1</sup> D. Flay,<sup>14</sup> S. Frullani,<sup>15</sup> F. Garibaldi,<sup>15</sup> H. Gao,<sup>16</sup> S. Gilad,<sup>17</sup> R. Gilman,<sup>1</sup> O. Glamazdin,<sup>18</sup> S. Golge,<sup>10</sup> J. Gomez,<sup>6</sup> O. Hansen,<sup>6</sup> D. W. Higinbotham,<sup>6</sup> T. Holmstrom,<sup>19</sup> J. Huang,<sup>17,20</sup> H. Ibrahim,<sup>21</sup> C. W. de Jager,<sup>6</sup> E. Jensen,<sup>22</sup> X. Jiang,<sup>20</sup> J. St. John,<sup>19</sup> M. Jones,<sup>6</sup> H. Kang,<sup>23</sup> J. Katich,<sup>8</sup> H. P. Khanal,<sup>9</sup> P. King,<sup>24</sup> W. Korsch,<sup>13</sup> J. LeRose,<sup>6</sup> R. Lindgren,<sup>5</sup> H.-J. Lu,<sup>25</sup> W. Luo,<sup>26</sup> P. Markowitz,<sup>9</sup> M. Mezziane,<sup>8</sup> R. Michaels,<sup>6</sup> B. Moffit,<sup>6</sup> P. Monaghan,<sup>11</sup> N. Muangma,<sup>17</sup> S. Nanda,<sup>6</sup> B. E. Norum,<sup>5</sup> K. Pan,<sup>17</sup> D. Parno,<sup>27</sup> E. Piasetzky,<sup>28</sup> M. Posik,<sup>14</sup> V. Punjabi,<sup>29</sup> A. J. R. Puckett,<sup>20</sup> X. Qian,<sup>16</sup> Y. Qiang,<sup>6</sup> X. Qiu,<sup>26</sup> S. Riordan,<sup>5</sup> G. Ron,<sup>30</sup> A. Saha,<sup>6,†</sup> B. Sawatzky,<sup>6</sup> R. Schiavilla,<sup>6,10</sup> B. Schoenrock,<sup>31</sup> M. Shabestari,<sup>5</sup> A. Shahinyan,<sup>32</sup> S. Širca,<sup>33,4</sup> R. Subedi,<sup>34</sup> V. Sulkosky,<sup>17</sup> W. A. Tobias,<sup>5</sup> W. Tireman,<sup>31</sup> G. M. Urciuoli,<sup>15</sup> D. Wang,<sup>5</sup> K. Wang,<sup>5</sup> Y. Wang,<sup>35</sup> J. Watson,<sup>6</sup> B. Wojtsekhowski,<sup>6</sup> Z. Ye,<sup>11</sup> X. Zhan,<sup>17</sup> Y. Zhang,<sup>26</sup> X. Zheng,<sup>5</sup> B. Zhao,<sup>8</sup> and L. Zhu<sup>11</sup>

(The Jefferson Lab Hall A Collaboration)

<sup>1</sup>*Rutgers University, New Brunswick, NJ 08901, USA*

<sup>2</sup>*University of Pennsylvania, Philadelphia, PA, 19104, USA*

<sup>3</sup>*Kent State University, Kent, OH 44242, USA*

<sup>4</sup>*Jožef Stefan Institute, SI-1000 Ljubljana, Slovenia*

<sup>5</sup>*University of Virginia, Charlottesville, VA 22908, USA*

<sup>6</sup>*Thomas Jefferson National Accelerator Facility, Newport News, VA 23606, USA*

<sup>7</sup>*Glasgow University, Glasgow G12 8QQ, Scotland, United Kingdom*

<sup>8</sup>*The College of William and Mary, Williamsburg, VA 23187, USA*

<sup>9</sup>*Florida International University, Miami, FL 33181, USA*

<sup>10</sup>*Old Dominion University, Norfolk, VA 23529, USA*

<sup>11</sup>*Hampton University, Hampton, VA 23669, USA*

<sup>12</sup>*Università degli studi di Bari Aldo Moro, I-70121 Bari, Italy*

<sup>13</sup>*University of Kentucky, Lexington, KY 40506, USA*

<sup>14</sup>*Temple University, Philadelphia, PA 19122, USA*

<sup>15</sup>*Istituto Nazionale Di Fisica Nucleare, INFN/Sanita, Roma, Italy*

<sup>16</sup>*Duke University, Durham, NC 27708, USA*

<sup>17</sup>*Massachusetts Institute of Technology, Cambridge, MA 02139, USA*

<sup>18</sup>*Kharkov Institute of Physics and Technology, Kharkov 61108, Ukraine*

<sup>19</sup>*Longwood University, Farmville, VA 23909, USA*

<sup>20</sup>*Los Alamos National Laboratory, Los Alamos, NM 87545, USA*

<sup>21</sup>*Cairo University, Cairo, Giza 12613, Egypt*

<sup>22</sup>*Christopher Newport University, Newport News VA 23606, USA*

<sup>23</sup>*Seoul National University, Seoul, Korea*

<sup>24</sup>*Ohio University, Athens, OH 45701, USA*

<sup>25</sup>*Huangshan University, People's Republic of China*

<sup>26</sup>*Lanzhou University, Lanzhou, Gansu, 730000, People's Republic of China*

<sup>27</sup>*Carnegie Mellon University, Pittsburgh, PA 15213, USA*

<sup>28</sup>*Tel Aviv University, Tel Aviv 69978, Israel*

<sup>29</sup>*Norfolk State University, Norfolk, VA 23504, USA*

<sup>30</sup>*Hebrew University of Jerusalem, Jerusalem 91904 Israel*

<sup>31</sup>*Northern Michigan University, Marquette, MI 49855, USA*

<sup>32</sup>*Yerevan Physics Institute, Yerevan, Armenia*

<sup>33</sup>*University of Ljubljana, SI-1000 Ljubljana, Slovenia*

<sup>34</sup>*George Washington University, Washington, D.C. 20052, USA*

<sup>35</sup>*University of Illinois at Urbana-Champaign, Urbana, IL 61801, USA*

We report the first measurement of the target single-spin asymmetry,  $A_y$ , in quasi-elastic scattering from the inclusive reaction  ${}^3\text{He}^\uparrow(e, e')$  on a  ${}^3\text{He}$  gas target polarized normal to the lepton scattering plane. Assuming time-reversal invariance, this asymmetry is strictly zero for one-photon exchange. A non-zero  $A_y$  can arise from the interference between the one- and two-photon exchange processes which is sensitive to the details of the sub-structure of the nucleon. An experiment recently completed at Jefferson Lab yielded asymmetries with high statistical precision at  $Q^2 = 0.13, 0.46$  and  $0.97 \text{ GeV}^2$ . These measurements demonstrate, for the first time, that the  ${}^3\text{He}$  asymmetry is clearly non-zero and negative at the  $(4\text{--}9)\sigma$  level. Using measured proton-to- ${}^3\text{He}$  cross-section

ratios and the effective polarization approximation, neutron asymmetries of  $-(1-3)\%$  were obtained. The neutron asymmetry at high  $Q^2$  is related to moments of the Generalized Parton Distributions (GPDs). Our measured neutron asymmetry at  $Q^2 = 0.97 \text{ GeV}^2$  agrees well with a prediction based on two-photon exchange using a GPD model and thus provides a new, independent constraint on these distributions.

PACS numbers: 24.70.+s, 14.20.Dh, 29.25.Pj

Elastic and inelastic form factors, extracted from electron-nucleon scattering data, provide invaluable information on nucleon structure. In most cases the scattering cross sections are dominated by one-photon exchange. Contributions from two-photon exchange are suppressed relative to the one-photon exchange contribution but are important in certain processes.

One observable that is exactly zero for one-photon exchange is the target-normal single-spin asymmetry (SSA),  $A_y$ , which is the focus of this experiment. When two-photon exchange is included,  $A_y$  can be non-zero. As shown in Fig. 1 the two photons form a loop that contains the nucleon intermediate state which has an elastic contribution that is calculable [1], and an inelastic contribution that must be modeled. This makes the two-photon exchange process sensitive to the details of nucleon structure and provides a powerful new tool for testing model predictions.

Recently,  $A_y$  for the neutron ( $^3\text{He}$ ) was measured to be non-zero and negative at the  $2.89\sigma$  level for deep-inelastic scattering [2]. A measurement of  $A_y$  in deep-inelastic scattering from polarized protons was consistent with zero at the  $\sim 10^{-3}$  level for  $Q^2 \geq 1 \text{ GeV}^2$  [3]. Two-photon-exchange contributions are also important when extracting the proton elastic form factor  $G_E^p(Q^2)$  from measured data at large  $Q^2$ . Values extracted from Rosenbluth separation of cross section data differ markedly from those extracted from polarization-transfer measurements [1, 4–8]. A GPD-based model prediction for the two-photon exchange contributions reduced the discrepancy by  $\sim 50\%$  for  $Q^2 \geq 2 \text{ GeV}^2$  [1]. This model was also used to predict  $A_y$ , thus providing an independent test in the absence of a large contribution from one-photon exchange. This paper presents the first measurement of  $A_y$  in quasi-elastic  $e$ - $n$  scattering, covering the range  $Q^2 = 0.1 - 1.0 \text{ GeV}^2$ . The precision data obtained at  $Q^2 = 1 \text{ GeV}^2$  will test the validity of the GPD-model and provide a constraint on the model input. The data at  $Q^2 = 0.13$  and  $0.46 \text{ GeV}^2$  can be used to test other calculations better suited for  $Q^2 < 1 \text{ GeV}^2$ .

Consider the elastic scattering of an unpolarized electron from a target nucleon with spin  $\vec{S}$ , oriented perpendicular (transversely polarized) to the incident electron 3-momentum  $\vec{k}$ , and normalized such that  $|\vec{S}| = 1$ . Our choice of coordinates is shown in Fig. 2 where  $\phi_S$  is the angle between the lepton plane and  $\vec{S}$  [2]. Requiring conservation of both the electromagnetic current and parity, the differential cross section,  $d\sigma$ , for the inclusive ( $e, e'$ )

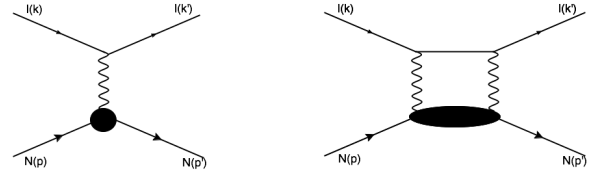


FIG. 1. In inclusive electron scattering a non-zero target-normal SSA can arise due to interference between one- (left) and two- (right) photon exchange. Here  $N$  is the nucleon with incident and outgoing 4-momenta  $p$  and  $p'$ , respectively, and  $l$  is the lepton with incident and outgoing 4-momenta  $k$  and  $k'$ , respectively. The intermediate nucleon state, represented by the black oval, includes both elastic and inelastic contributions and is thus sensitive to the structure of the nucleon.

reaction is written as [9–11]

$$\begin{aligned} d\sigma(\phi_S) &= d\sigma_{UU} + \frac{\vec{S} \cdot (\vec{k} \times \vec{k}')}{|\vec{k} \times \vec{k}'|} d\sigma_{UT} \\ &= d\sigma_{UU} + d\sigma_{UT} \sin \phi_S, \end{aligned} \quad (1)$$

where  $\vec{k}'$  is the 3-momentum of the scattered electron, and  $d\sigma_{UU}$  and  $d\sigma_{UT}$  are the cross sections for an unpolarized electron scattered from an unpolarized and transversely polarized target, respectively. The target SSA is defined as

$$A_{UT}(\phi_S) = \frac{d\sigma(\phi_S) - d\sigma(\phi_S + \pi)}{d\sigma(\phi_S) + d\sigma(\phi_S + \pi)} = A_y \sin \phi_S. \quad (2)$$

By measuring  $A_{UT}$  at  $\phi_S = \pi/2$  one can extract the quantity  $A_y \equiv \frac{d\sigma_{UT}}{d\sigma_{UU}}$ , which is the SSA for a target polarized normal to the lepton scattering plane.

For one-photon exchange we can write  $d\sigma_{UU} \propto \text{Re}(\mathcal{M}_{1\gamma}\mathcal{M}_{1\gamma}^*)$  and  $d\sigma_{UT} \propto \text{Im}(\mathcal{M}_{1\gamma}\mathcal{M}_{1\gamma}^*)$ , where  $\mathcal{M}_{1\gamma}$  is the one-photon exchange amplitude and  $\text{Re}$  ( $\text{Im}$ ) stands for the real (imaginary) part. However, time-reversal invariance requires that  $\mathcal{M}_{1\gamma}$  be real and so at order  $\alpha^2$ ,  $d\sigma_{UU}$  can be non-zero, but  $d\sigma_{UT}$  must be zero [9]. When one includes the (complex) two-photon exchange amplitude,  $\mathcal{M}_{2\gamma}$ , the contribution to the asymmetry from the interference between one- and two-photon exchange amplitudes is  $d\sigma_{UT} \propto \text{Im}(\mathcal{M}_{1\gamma}\mathcal{M}_{2\gamma}^*)$  which can be non-zero at order  $\alpha^3$ .

Using the formalism of Ref. [1], we can write

$$A_y = \sqrt{\frac{2\varepsilon(1+\varepsilon)}{\tau}} \frac{1}{\sigma_R} \left\{ -G_M \text{Im} \left( \delta\tilde{G}_E + \frac{\nu'}{M^2} \tilde{F}_3 \right) + G_E \text{Im} \left( \delta\tilde{G}_M + \left( \frac{2\varepsilon}{1+\varepsilon} \right) \frac{\nu'}{M^2} \tilde{F}_3 \right) \right\}, \quad (3)$$

where  $\tau \equiv Q^2/4M^2$ ,  $\nu' = \frac{1}{4}(k_\mu + k'_\mu)(p^\mu + p'^\mu)$ ,  $\varepsilon \equiv (1 + 2(1 + \tau) \tan^2 \frac{\theta}{2})^{-1}$  and  $M$  is the mass of the nucleon. In the lab frame,  $E$ ,  $E'$  and  $\theta$  are the incident and scattered energies, and scattering angle, of the electron, respectively. The  $G_E$  and  $G_M$  are the Sachs form factors and  $\sigma_R$  is the reduced unpolarized cross section. The terms  $\delta\tilde{G}_E$ ,  $\delta\tilde{G}_M$  and  $\tilde{F}_3$  are additional complex contributions that arise when two-photon exchange is included. They are exactly zero for one-photon exchange. For the neutron, unlike the proton,  $G_E \ll G_M$  so that Eq. (3) is dominated by the term proportional to  $G_M$ . Note that the unpolarized cross section and polarization transfer observables depend on the real parts of  $\delta\tilde{G}_E$ ,  $\delta\tilde{G}_M$  and  $\tilde{F}_3$ .

For  $Q^2 \geq 1 \text{ GeV}^2$  the two-photon contributions to Eq. (3) were estimated using weighted moments of the GPDs,  $H^q$ ,  $E^q$  and  $\tilde{H}^q$ , for a quark  $q$  [1]. For lower  $Q^2$ ,  $A_y$  can be estimated using e.g. model fits of nucleon resonance and pion production data [7, 12]. However, there are no predictions in the kinematic range of this experiment. The only existing measurement was made on the proton at SLAC in 1970 [13]. They measured asymmetries at  $Q^2 = 0.38, 0.59$  and  $0.98 \text{ GeV}^2$  that were consistent with zero at the  $\sim 10^{-2}$  level. There has never been a measurement made on the neutron.

This paper presents the results of Jefferson Lab experiment E05-015, which measured  $A_y$  by scattering unpolarized electrons from  $^3\text{He}$  nuclei polarized normal to the electron scattering plane. The electron beam was longitudinally polarized with energies of 1.2, 2.4 and 3.6 GeV and an average current of  $12 \mu\text{A}$  (CW). The helicity of the beam was flipped at a rate of 30 Hz (for other experiments requiring a polarized electron beam) and data from the two helicity states were summed for this analysis.

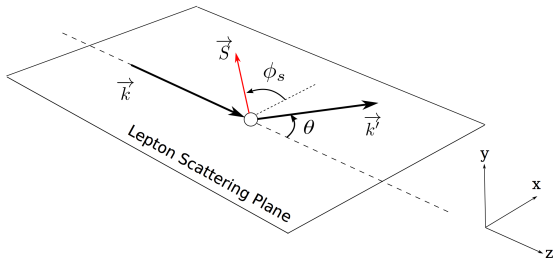


FIG. 2. Coordinate system used to define  $A_{UT}(\phi_S)$ . Note that  $\vec{S}$  is perpendicular to  $\hat{z}$ .

The polarized target used in this experiment was a 40

cm-long aluminosilicate glass cell filled with  $^3\text{He}$  gas at a density of 10.9 amg. Approximately 0.1 amg of  $\text{N}_2$  gas was also included to aid in the polarization process. The target was polarized through spin-exchange optical pumping of a Rb-K mixture [14]. In order to reduce the systematic uncertainty, the direction of the target polarization vector was reversed every 20 minutes using adiabatic fast passage. The polarization was monitored during each spin-flip using nuclear magnetic resonance. Electron paramagnetic resonance measurements were periodically made throughout the experiment in order to calibrate the polarization [15]. The average in-beam target polarization was  $(51.4 \pm 2.9)\%$ .

The electron beam was rastered in a  $3 \text{ mm} \times 3 \text{ mm}$  pattern to reduce the possibility of cell rupture due to localized heating of the thin glass windows. Electrons scattered from the target were detected using the two Hall A high resolution spectrometers (HRSeS) [16] at scattering angles  $\theta = \pm 17^\circ$ , consistent with Figure 2. Because the out-of-plane acceptance of the spectrometers is relatively small,  $\pm 60 \text{ mrad}$ , the correction for  $\phi_S \neq \pm \pi/2$  is negligible. We define the  $+\hat{y}$  direction as “target spin up” ( $\uparrow$ ) and the  $-\hat{y}$  direction as “target spin down” ( $\downarrow$ ). Both spectrometers were configured to detect electrons in single-arm mode using nearly identical detector packages, each consisting of two dual-plane vertical drift chambers for tracking, two planes of segmented plastic scintillator for trigger formation, and  $\text{CO}_2$  gas Cherenkov and Pb-glass electromagnetic calorimeter detectors for hadron rejection. The data acquisition systems for the spectrometers were synchronized to allow cross-checking of the results. By simultaneously measuring with two independent spectrometers, we confirmed that the measured asymmetries were consistent in magnitude, with opposite signs, as expected.

The electron yields,  $Y^{\uparrow(\downarrow)}$ , give the number of electrons ( $N^{\uparrow(\downarrow)}$ ) in the target spin-up (spin-down) state that pass all the particle-identification cuts, normalized by accumulated beam charge ( $Q^{\uparrow(\downarrow)}$ ) and data-acquisition live-time ( $LT^{\uparrow(\downarrow)}$ ):

$$Y^{\uparrow(\downarrow)} = \frac{N^{\uparrow(\downarrow)}}{Q^{\uparrow(\downarrow)} \cdot LT^{\uparrow(\downarrow)}} \quad (4)$$

The raw experimental asymmetries were calculated as

$$A_{\text{raw}} = \frac{Y^\uparrow - Y^\downarrow}{Y^\uparrow + Y^\downarrow} \quad (5)$$

and were corrected for nitrogen dilution and target polarization. The nitrogen dilution factor is defined as

$$f_{\text{N}_2} \equiv \frac{\rho_{\text{N}_2} \sigma_{\text{N}_2}}{\rho_{^3\text{He}} \sigma_{^3\text{He}} + \rho_{\text{N}_2} \sigma_{\text{N}_2}}, \quad (6)$$

where  $\rho_i$  and  $\sigma_i$  are the number densities and unpolarized cross sections, respectively. The nitrogen density was measured when filling the target cell and the cross-section

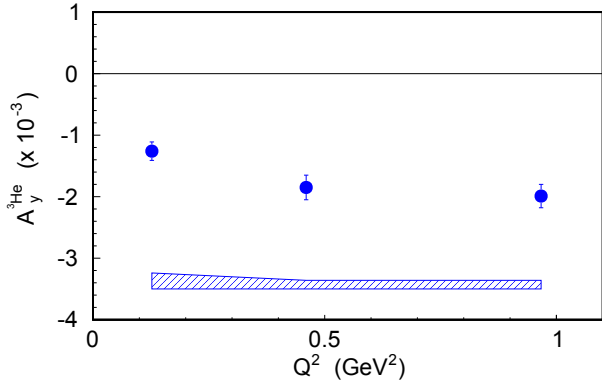


FIG. 3. Measured  $^3\text{He}$  asymmetries,  $A_y^{^3\text{He}}$ , as a function of  $Q^2$ . Uncertainties shown on the data points are statistical. Systematic uncertainties are shown by the band at the bottom.

was determined experimentally by electrons scattering from a reference cell filled with a known quantity of  $\text{N}_2$ . The denominator was obtained from the polarized target cell yields.

The final asymmetries were obtained after subtraction of the elastic radiative tail contribution, radiative corrections of the quasi-elastic asymmetries and corrections for bin-averaging effects. The contribution of the elastic radiative tail to the lowest  $Q^2$  point was 3%, and was negligible for the two larger  $Q^2$  points. At the lower two values of  $Q^2$ , contamination from the tail of the  $\Delta$  resonance is negligible. At  $Q^2 = 0.97 \text{ GeV}^2$ , the contamination from the  $\Delta$  tail can become large depending on the choice of cut in  $\nu = E - E'$ . However, our measured  $A_y^{^3\text{He}}$  showed no dependence on  $\nu$ , within our statistical precision.

Results for  $A_y^{^3\text{He}}$  are shown in Fig. 3 and listed in Table I. The uncertainties on the data points are statistical, with the total experimental systematic uncertainty indicated as an error band below the data points. The systematic uncertainty in  $A_y^{^3\text{He}}$  includes contributions from the live-time asymmetry, target polarization, target misalignment, nitrogen dilution and radiative corrections. The dominant contribution to the systematic uncertainty at the two largest  $Q^2$  points is the uncertainty in the target polarization,  $\pm 5.6\%$  (rel.). At the two largest  $Q^2$  points, the results from the left and right HRS agree to  $< 1\sigma$  (stat.). At the lowest  $Q^2$  point we assign a systematic uncertainty of  $\pm 2.4 \times 10^{-4}$  because the data from the two spectrometers differ by  $\sim 2\sigma$  (stat.).

Polarized  $^3\text{He}$  targets have been used in many experiments as an effective polarized neutron target [17, 18]. The ground state of the  $^3\text{He}$  nucleus is dominated by the  $S$ -state in which the two proton spins are anti-parallel, and the nuclear spin is carried by the neutron [19]. From the polarized  $^3\text{He}$  asymmetries, the neutron asymmetries,  $A_y^n$ , were extracted using the effective neutron polariza-

tion approximation [20],

$$A_y^n = \frac{1}{f_n P_n} (A_y^{^3\text{He}} - (1 - f_n) P_p A_y^p). \quad (7)$$

The neutron dilution factor is the ratio of the neutron to  $^3\text{He}$  unpolarized elastic cross sections,  $f_n = \sigma_n / \sigma_{^3\text{He}}$ . At the lowest value of  $Q^2$ , where nuclear effects may be important,  $f_n$  was calculated using a non-relativistic model of the  $^3\text{He}$  nucleus from A. Deltuva [21–24] based on the CD-Bonn +  $\Delta$  potential. The model uncertainty is 3.8% (rel.) based on a study of the model dependence of  $f_n$  at  $Q^2 \approx 1 \text{ GeV}^2$  in a previous  $^3\text{He}(e, e')$  measurement by this collaboration [25].

For neutron asymmetries at  $Q^2 = 0.46$  and  $0.97 \text{ GeV}^2$ , the  $f_n$  were obtained using the assumption  $f_n = \sigma_n / (2\sigma_p + \sigma_n)$ , where  $\sigma_p$  is the unpolarized proton elastic cross section. Reduced cross sections were calculated using

$$\sigma_R(Q^2) = \tau G_M^2(Q^2) + \epsilon G_E^2(Q^2) \quad (8)$$

The form factors  $G_E^p$ ,  $G_M^p$ ,  $G_E^n$  and their uncertainties were obtained from parameterizations by Kelly [26]. A parameterization by Qattan and Arrington [27] was used to obtain  $G_M^n$  and its uncertainty.

The effective neutron and proton polarizations in  $^3\text{He}$  are  $P_n = 0.86 \pm 0.036$  and  $P_p = -0.028 \pm 0.009$ , respectively [28]. In lieu of precision data, the proton asymmetries,  $A_y^p$ , were estimated using the elastic intermediate state contributions to be  $(0.01 \pm 0.22)\%$ ,  $(0.24 \pm 2.96)\%$  and  $(0.62 \pm 1.09)\%$  for the data at  $Q^2 = 0.13$ ,  $0.46$  and  $0.97 \text{ GeV}^2$ , respectively [29]. The uncertainties in these values were calculated assuming the same relative differences as those seen between our measured neutron asymmetries and the neutron elastic contribution. The contributions to Eq. (7) from  $A_y^p$  are suppressed by the small effective proton polarization,  $P_p$ , in polarized  $^3\text{He}$ . The neutron single-spin asymmetries are shown in Fig. 4 and listed in Table I along with values for  $f_n$ .

In summary, we have reported the first measurement of the target single-spin asymmetries,  $A_y$ , from quasi-elastic  $(e, e')$  scattering from a  $^3\text{He}$  target polarized normal to the electron scattering plane. This measurement demonstrates, for the first time, that the  $^3\text{He}$  asymmetries are clearly non-zero and negative at the  $(4 - 9)\sigma$  level. Neutron asymmetries were extracted using the effective neutron polarization approximation and are also clearly non-zero and negative. The results are inconsistent with an estimate where only the elastic intermediate state is included [29] but are consistent with a model using GPD input for the inelastic intermediate state contribution at  $Q^2 = 0.97 \text{ GeV}^2$  [1].

We acknowledge the outstanding support of the Jefferson Lab Hall A technical staff and Accelerator Division in accomplishing this experiment. We wish to thank Drs. A. Deltuva, Vilnius Univ., A. Afanasev, Jefferson

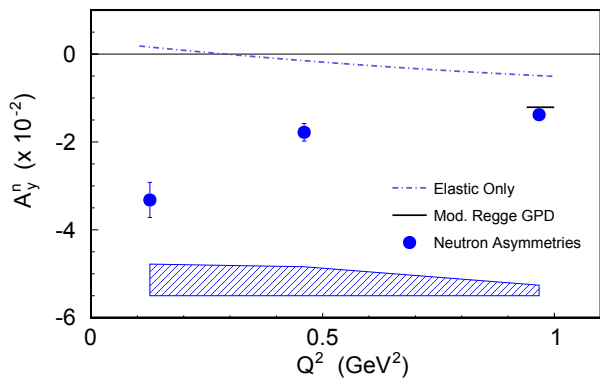


FIG. 4. Results for the neutron asymmetries,  $A_y^n$ , as a function of  $Q^2$ . Uncertainties shown on the data points are statistical. Systematic uncertainties are shown by the band at the bottom. The elastic contribution to the intermediate state is shown by the dot-dash line [29], and at  $Q^2 = 0.97 \text{ GeV}^2$ , the GPD calculation of Chen *et al.* [1] is shown by the short solid line.

Lab, M. Vanderhaeghen, MAINZ and J. Arrington, Argonne National Lab for theoretical guidance and calculations. This work was supported in part by the U.S. National Science Foundation, the U.S. Department of Energy and by DOE contract DE-AC05-06OR23177, under which Jefferson Science Associates, LLC operates the Thomas Jefferson National Accelerator Facility, the National Science Foundation of China and UK STFC grants 57071/1, 50727/1.

\* Corresponding author: tdaver@wm.edu

† Deceased.

- [1] Y. Chen, A. Afanasev, S. Brodsky, C. Carlson, and M. Vanderhaeghen, Phys. Rev. Lett. **93**, 122301 (2004).
- [2] J. Katich, X. Qian, Y. Zhao, K. Allada, K. Aniol, *et al.*, Phys. Rev. Lett. **113**, 022502 (2014), arXiv:1311.0197 [nucl-ex].
- [3] A. Airapetian *et al.* (HERMES Collaboration), Phys. Lett. B **682**, 351 (2010), arXiv:0907.5369 [hep-ex].
- [4] J. Arrington, Phys. Rev. C **68**, 034325 (2003).
- [5] J. Arrington, P. Blunden, and W. Melnitchouk, Prog.

- Part. Nucl. Phys. **66**, 782 (2011), arXiv:1105.0951 [nucl-th].
- [6] A. Puckett, E. Brash, O. Gayou, M. Jones, L. Pentchev, *et al.*, Phys. Rev. C **85**, 045203 (2012).
- [7] P. G. Blunden, W. Melnitchouk, and J. A. Tjon, Phys. Rev. Lett. **91**, 142304 (2003).
- [8] C. E. Carlson and M. Vanderhaeghen, Annu. Rev. Nucl. Part. Sci. **57**, 171 (2007).
- [9] N. Christ and T. D. Lee, Phys. Rev. **143**, 1310 (1966).
- [10] R. N. Cahn and Y. S. Tsai, Phys. Rev. D **2**, 870 (1970).
- [11] A. Afanasev, M. Strikman, and C. Weiss, Phys. Rev. D **77**, 014028 (2008).
- [12] B. Pasquini and M. Vanderhaeghen, Phys. Rev. C **70**, 045206 (2004), arXiv:hep-ph/0405303 [hep-ph].
- [13] T. Powell, M. Borghini, O. Chamberlain, R. Z. Fuzesy, C. C. Morehouse, *et al.*, Phys. Rev. Lett. **24**, 753 (1970).
- [14] J. Singh, P. Dolph, W. Tobias, T. Averett, A. Kelleher, *et al.*, Phys. Rev. C **91**, 055205 (2015), arXiv:1309.4004 [physics.atom-ph].
- [15] M. V. Romalis and G. D. Cates, Phys. Rev. A **58**, 3004 (1998).
- [16] J. Alcorn, B. Anderson, K. Aniol, J. Annand, L. Auerbach, *et al.*, Nucl. Instrum. Meth. A **522**, 294 (2004).
- [17] S. Kuhn, J.-P. Chen, and E. Leader, Prog. Part. Nucl. Phys. **63**, 1 (2009), arXiv:0812.3535 [hep-ph].
- [18] X. Qian *et al.* (Jefferson Lab Hall A Collaboration), Phys. Rev. Lett. **107**, 072003 (2011), arXiv:1106.0363 [nucl-ex].
- [19] F. Bissey, V. Guzey, M. Strikman, and A. Thomas, Phys. Rev. C **65**, 064317 (2002).
- [20] S. Scopetta, Phys. Rev. D **75**, 054005 (2007).
- [21] A. Deltuva, R. Machleidt, and P. Sauer, Phys. Rev. C **68**, 024005 (2003).
- [22] A. Deltuva, L. Yuan, J. Adam, A. Fonseca, and P. Sauer, Phys. Rev. C **69**, 034004 (2004).
- [23] A. Deltuva, L. Yuan, J. Adam, and P. Sauer, Phys. Rev. C **70**, 034004 (2004).
- [24] A. Deltuva, A. Fonseca, and P. Sauer, Phys. Rev. C **72**, 054004 (2005).
- [25] W. Xu, D. Dutta, F. Xiong, B. Anderson, L. Auerbach, *et al.*, Phys. Rev. Lett. **85**, 2900 (2000), arXiv:nucl-ex/0008003 [nucl-ex].
- [26] J. J. Kelly, Phys. Rev. C **70**, 068202 (2004).
- [27] I. Qattan and J. Arrington, Phys. Rev. C **86**, 065210 (2012), J. Arrington, *private communication*.
- [28] X. Zheng *et al.* (Jefferson Lab Hall A Collaboration), Phys. Rev. Lett. **92**, 012004 (2004).
- [29] A. Afanasev, I. Akushevich, and N. Merenkov, (2002), arXiv:hep-ph/0208260 [hep-ph].

$E$ (GeV)	$\langle E' \rangle$ (GeV)	$\langle \theta \rangle$ (deg.)	$\langle Q^2 \rangle$ (GeV <sup>2</sup> )	$A_y^{^3\text{He}} (\times 10^{-3})$	$A_y^n (\times 10^{-2})$	$f_n$
1.245	1.167	17	0.127	$-1.26 \pm 0.15 \pm 0.26$	$-3.32 \pm 0.40 \pm 0.72$	$0.044 \pm 0.002$
2.425	2.170	17	0.460	$-1.85 \pm 0.20 \pm 0.14$	$-1.78 \pm 0.20 \pm 0.66$	$0.117 \pm 0.003$
3.605	3.070	17	0.967	$-1.99 \pm 0.19 \pm 0.14$	$-1.38 \pm 0.14 \pm 0.24$	$0.155 \pm 0.007$

TABLE I. Asymmetries,  $A_y$ , for  $^3\text{He}$  and neutrons. Uncertainties are statistical and systematic, respectively. The systematic uncertainty in the neutron asymmetry includes the model uncertainty in the neutron dilution factor  $f_n$ , also listed here.